Truncated KCNQ1 mutant, A178fs/105, forms hetero-multimer channel with wild-type causing a dominant-negative suppression due to trafficking defect

Yoshiyasu Aizawa[a,b], Kazuo Ueda[c], Long-mei Wu[a], Natsuko Inagaki[c], Takeharu Hayashi[c], Megumi Takahashi[c], Masaaki Ohta[d], Seiko Kawano[a], Yuji Hirano[a], Michio Yasunami[c], Yoshifusa Aizawa[b], Akinori Kimura[c], Masayasu Hiraoka[a,*]

[a] *Department of Cardiovascular Diseases, Medical Research Institute, Tokyo Medical and Dental University, 1-5-45 Yushima, Bunkyo-ku, Tokyo 113-8510, Japan*
[b] *Division of Cardiology, Niigata University Graduate School of Medical and Dental Sciences, 1-757 Asahimachi-dori, Niigata-shi, Niigata 951-8510, Japan*
[c] *Department of Molecular Pathogenesis, Medical Research Institute, Tokyo Medical and Dental University, 2-3-10 Kanda-Surugadai, Chiyoda-ku, Tokyo 113-8510, Japan*
[d] *Department of Pediatrics, Ehime Prefectural Imabari Hospital, 4-5-5 Ishii-cho, Imabari-shi, Ehime 794-0006, Japan*

Received 21 June 2004; revised 28 July 2004; accepted 5 August 2004

Available online 21 August 2004

Edited by Felix Wieland

Abstract **We identified a novel mutation Ala178fs/105 missing S3–S6 and C-terminus portions of KCNQ1 channel. Ala178fs/105-KCNQ1 expressed in COS-7 cells demonstrated no current expression. Co-expression with wild-type (WT) revealed a dominant-negative effect, which suggests the formation of hetero-multimer by mutant and WT. Confocal laser microscopy displayed intracellular retention of Ala178fs/105-KCNQ1 protein. Co-expression of the mutant and WT also increased intracellular retention of channel protein compared to WT alone. Our findings suggest a novel mechanism for LQT1 that the truncated S1–S2 KCNQ1 mutant forms hetero-multimer and cause a dominant-negative effect due to trafficking defect.**

Keywords: KCNQ1 (KvLQT1); Frameshift mutation; Membrane trafficking; Electrophysiology; Sudden cardiac death

1. Introduction

Long QT syndrome (LQTS) is characterized by QT prolongation, syncope, and sudden cardiac death due to polymorphic ventricular tachyarrhythmias. Mutations in *KCNQ1* gene cause the most frequent form long QT syndrome type 1 (LQT1) of inherited LQTS. So far, more than 100 mutations have been identified and various mechanisms of channel dysfunction are implicated [1]. Among the factors causing channel dysfunction, trafficking defect of channel protein in *KCNQ1* is rare as compared to the cases of *KCNH2* (*HERG*) mutations. We identified several novel mutations in *KCNQ1* and *KCNH2* from Japanese LQTS patients. One of the patients who showed severe phenotype disclosed a frameshift mutation resulting in the truncation of KCNQ1 channel to the S1–S2 portion. We evaluated functional properties of this frameshift mutation expressed in COS-7 cells.

* Corresponding author. Fax: +81-3-5684-6295.
E-mail address: hiraoka-masayasu@mhlw.go.jp (M. Hiraoka).

Abbreviations: LQTS, long QT syndrome; LQT1, long QT syndrome type 1; ECG, electrocardiogram; DNA, deoxyribonucleic acid; PCR, polymerase chain reaction; SSCP, single-strand conformation polymorphism; WT, wild-type; cDNA, complementary deoxyribonucleic acid; CFP, cyan fluorescent protein; YFP, yellow fluorescent protein; S.E.M., standard error of mean

2. Materials and methods

2.1. A case presentation

A 13-year-old girl was referred to our institute for genetic analysis. She had a history of cardiopulmonary arrest while during swimming in the pool. Her hearing ability was normal and she had no family history of syncope or sudden cardiac death. Her electrocardiogram (ECG) showed broad-based and high amplitude T wave. QTc interval at baseline was 0.52 s (Fig. 1) and it further prolonged with exercise up to 0.62 s. The β-blocking drug, propranolol, is effective in suppressing recurrent arrhythmic events.

2.2. Genetic analysis

The study was approved by the Ethics Reviewing Committee of Medical Research Institute, Tokyo Medical and Dental University. After written informed consent was obtained, the genomic deoxyribonucleic acid (DNA) was isolated from peripheral blood lymphocytes by conventional methods. The genomic DNA was amplified on GeneAmp^{R} PCR System 9700 thermal cycler by standard polymerase chain reaction (PCR) technique using the primers as described previously [2]. For the genetic screening, we used single-strand conformation polymorphism (SSCP) followed by DNA sequencing method as for *KCNQ1*, *KCNH2*, *SCN5A*, *KCNE1* and *KCNE2* genes. Abnormal conformers were sequenced with ABI377XL genetic analyzer (Applied Biosystems). Electropherograms were compared with the *KCNQ1* wild-type (WT) sequence (GenBank Accession No. AJ006343) using the DNASIS Ver. 3.7 software (HITACHI). Genetic screening for her family members was not available.

2.3. Wild type- and mutant-KCNQ1 constructs

The WT *KCNQ1* and *KCNE1* complementary deoxyribonucleic acids (cDNAs) were amplified from the adult heart cDNA of Human Cardiovascular MTC Panel^{TM} (BD Biosciences Clontech) by PCR using primer pairs; KCNQ1-forward/reverse (5′-GGATCCGTT-

0014-5793/$22.00 © 2004 Published by Elsevier B.V. on behalf of the Federation of European Biochemical Societies.
doi:10.1016/j.febslet.2004.08.018

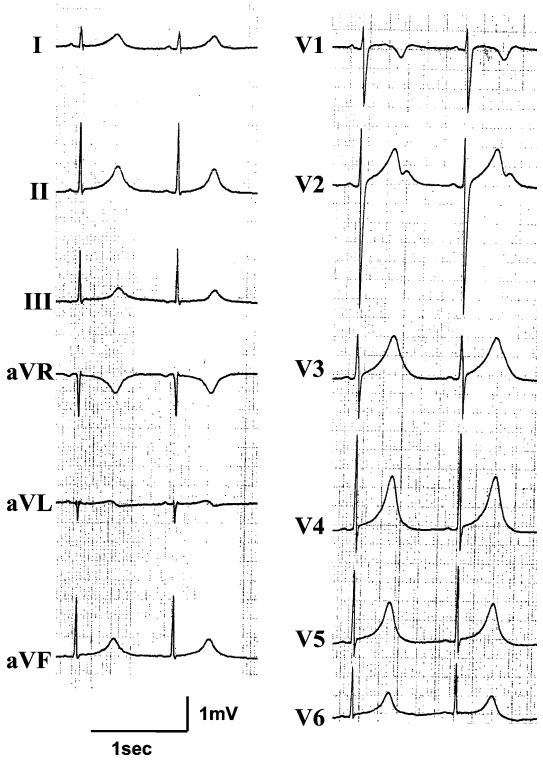

Fig. 1. ECG of the patient at rest. QTc interval was prolonged to 0.52 s.

ATGGCCGCGGCCTCCTC-3′ and 5′-GCCTCCCTCTCACTCAGGCCCTCC-3′) and KCNE1-forward/reverse (5′-CAGGATGATCCTGTCTAACACC-3′ and 5′-GGATCCTCATGGGGAAGGCTTCGT-3′), respectively (artificial BamHI sites and the initiation codons are underlined). The PCR products were cloned into pCR2.1 vector (Invitrogen CA). The substitution of GG for C found in the Ala178fs/105 (A178fs/105) mutant-*KCNQ1* was introduced to WT-*KCNQ1* cDNA by overlap extension using the PCR [3]. In brief, the mutagenic oligonucleotides for the A178fs/105 substitution are A178fs-forward (5′-TCTGGTCCGGGCGGCTGCCGCA-3′) and A178fs-reverse (5′-TGCGGCAGCCGCCCGGACCAGA-3′, underlines indicate the site of mutation). The two PCR products with KCNQ1-forward and A178fs-reverse primers and A178fs-forward and A178fs-reverse (5′-TCTAGACTCGTTCACCGCGTCCTTCT-3′, *Xba*I site added is underlined) primers were mixed and subjected to ligation PCR using flanking primers, KCNQ1-forward and A178fs-reverse. The resultant PCR fragment, which spans from the initiation codon to the premature termination codon, appeared in the mutant at position +105 and was cloned into pCR2.1 vector. For electrophysiological studies, the *Bam*HI–*Eco*RI fragment containing WT- or mutant-*KCNQ1* coding sequence was excised from the corresponding pCR2.1 cDNA clone and inserted to an expression vector pcDNA3.1(+) (Invitrogen). For confocal microscopic analysis, *Bam*HI–*Xba*I fragment of cDNA clone was ligated to *Bam*HI–*Xba*I cleaved cyan fluorescent protein (CFP) or yellow fluorescent protein (YFP) expression vector pECFP-C1 or pEYFP-C1 (BD Biosciences Clonetech). For *KCNE1* cDNA expression, *Bam*HI–*Eco*RI fragment of the cDNA clone was inserted into pcDNA3.1(+) expression vector. All the inserts of plasmid vectors used in this study were sequenced to ensure that no PCR error was introduced.

2.4. Cell culture and transient transfection

A cell line COS-7 was obtained from American Type Cell Collection and cultured in Dulbecco's modified Eagle's medium (Invitrogen) supplemented with 10% fetal bovine serum and 1% penicillin–streptomycin in a humidified 5% CO_2 incubator at 37 °C. Cultured cells were seeded in 60-mm dishes 1 day before transfection and transiently transfected with various plasmids by lipofectamine method using the SuperFect Transfection Reagent (QIAGEN). In the electrophysiologic experiments, 1.25 or 0.625 μg of WT-*KCNQ1* (cloned into pcDNA3.1), 0.625 μg WT- and 0.625 μg mutant-*KCNQ1* (cloned into pcDNA3.1), and 1.25 μg mutant-*KCNQ1* were used alone with the same amount of *KCNE1* (cloned into pcDNA3.1). pEGFP-C1 was co-transfected to allow for identification of the transfected cells. Cells displaying green fluorescence 24–48 h after transfection were used for the electrophysiologic experiments.

2.5. Electrophysiological recordings

Whole-cell patch-clamp method was applied to COS-7 cells transfected with WT- and/or mutant-*KCNQ1* channel as described previously [4]. Briefly, cells were allowed to settle on the bottom of bath (0.5 mL) mounted on an inverted microscope (Diaphoto TMD, Nikon). Cells were superfused with normal Tyrode's solution containing (in mmol/L) 144 NaCl, 0.33 NaH_2PO_4, 4 KCl, 1.8 $CaCl_2$, 0.53 $MgCl_2$, 5.5 Glucose and 5.0 HEPES (pH 7.4 adjusted with NaOH). The glass pipettes had an inner diameter of ~1.0–1.5 μm andd resistance of 2–3 MΩ when filled with the internal solution. The internal solution contained (in mmol/L) 100 K-aspartate, 20 KCl, 5 ATP-Mg, 5CP-K_2, 5 EGTA, 5 HEPES and 1 $CaCl_2$ (pH 7.2 adjusted with KOH). A patch-clamp amplifier (Axopatch 200B, Axon Instruments) was used to record membrane currents. After forming a whole-cell configuration, cell membrane capacitance was estimated by analyzing capacity transient elicited by 5 mV hyperpolarizing pulses. Series resistance compensation was done by 50–70% using the circuit built into the amplifier (Axopatch 200B). Cells were held at holding potential of −80 mV and depolarizing pulses to various potentials ranging from −40 to +70 mV in 10 mV increments for 7.5 s were applied followed by repolarization to −50 mV for 2 s to record tail currents. Software (pCLAMP 8.0, Axon Instruments) was used to generate pulse protocol, data acquisition and analysis. All experiments were done at room temperature (22–24 °C).

2.6. Confocal microscopy

CFP-tagged WT-*KCNQ1* and YFP-tagged mutant-*KCNQ1* were transfected to COS-7 cells in glass-bottomed well slide (Lab-Tek). Forty-eight hours after the transfection, cells were fixed on slide-glass with 4% paraformaldehyde and visualized using LSM510 confocal laser scanning microscope (Carl Zeiss). Argon laser was used to excite the CFP (excitation wavelength = 458 nm) and YFP (excitation wavelength = 514 nm). CFP fluorescence was detected with the BP465/495 filter set and assigned as blue. YFP fluorescence was detected with the BP535/565 filter set and assigned as yellow. Merged image was obtained by overlaying images from individual channels using LSM510 confocal laser scanning microscope was assigned as white.

2.7. Data analysis

All data were expressed as means ± S.E.M. Student's t test was performed for statistical evaluation. $P < 0.05$ was considered significant.

3. Results

3.1. Mutational analysis

Abnormal bands were detected by the SSCP method in exon 3 of *KCNQ1* (Fig. 2A) . The sequence of abnormal fragment revealed a substitution of GG for C at position 533 in *KCNQ1* (Fig. 2B). This abnormal sequence causes a reading frameshift at amino acid 178 alanine resulting in shortened open reading frame, with additional 105 out of frame amino acid residues (Ala178fs/105), thereby eliminating the portions of S3–S6 and C-terminus of KCNQ1 channel (Fig. 2C). This mutation was not detected in blood samples from 150 unrelated healthy Japanese individuals.

3.2. Electrophysiological properties of mutant-KCNQ1 currents

The cells transfected with 1.25 μg of WT-*KCNQ1* together with 1.25 μg of *KCNE1* exhibited slowly activating outward current compatible with I_{Ks} in native cardiac myocytes

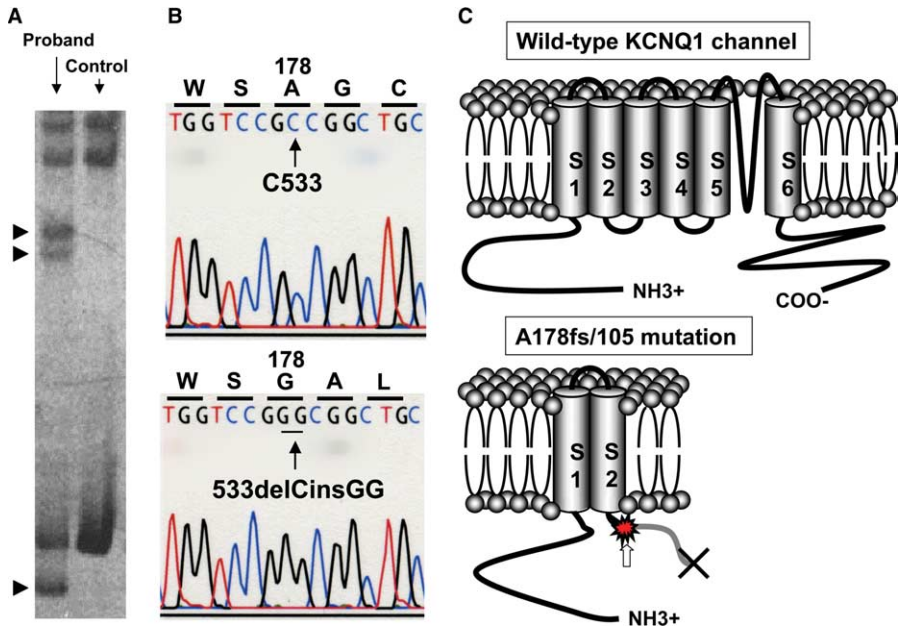

Fig. 2. SSCP and electropherogram. (A) SSCP analysis detected abnormal band in the exon 3 of *KCNQ1*. (B) Electropherogram after sequencing of index patient. A heterozygous C to GG transposition at the position of 533 nucleotides was confirmed. (C) Schematic topology of *KCNQ1* channels. Because of the frameshift in the S2–S3 cytoplasmic loop, resulting premature stop codon deleted the S3–S6 including pore region and C-termini and being replaced by additional 105 out of frame amino acid residues (thick gray line).

(Fig. 3B), while the mutant-*KCNQ1* with the same amount of *KCNE1* did not produce any currents (Fig. 3D). The cells transfected with 0.625 μg of WT-*KCNQ1* (+*KCNE1*) expressed the currents of nearly half amplitude of those with 1.25 μg of WT-*KCNQ1* (Fig. 3B). The co-expression of 0.625 μg of WT-*KCNQ1* with the same amount of mutant-*KCNQ1* (+ *KCNE1*)

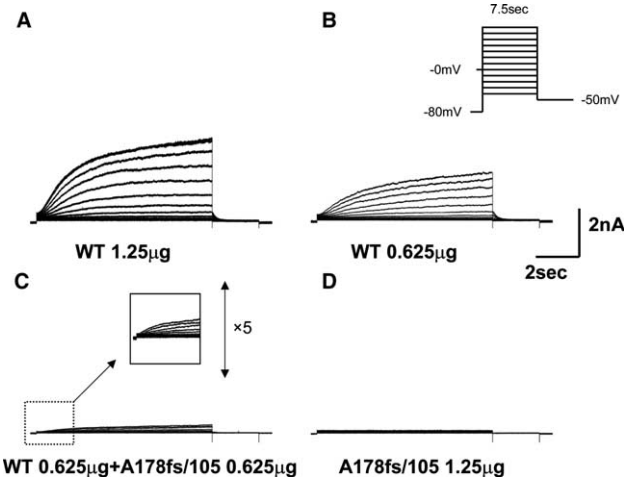

Fig. 3. Representative current trace of WT- and/or A178fs/105 mutant-*KCNQ1* expressed in COS-7 cells. Cells of each panel were transfected as follows: (A) 1.25 μg of WT-*KCNQ1*/pcDNA3.1(+) and 1.25 μg of *KCNE1*/pcDNA3.1(+), (B) 0.625 μg of WT-*KCNQ1*/pcDNA3.1(+) and 0.625 μg of *KCNE1*/pcDNA3.1(+), (C) 0.625 μg of WT-*KCNQ1*/pcDNA3.1(+), 0.625 μg of A178fs/105 mutant-*KCNQ1* /pcDNA3.1(+) and 1.25 μg of *KCNE1*/pcDNA3.1(+). The initial portion of the current traces (dashed square) was enlarged in the solid square. (D) 1.25 μg of A178fs/105 mutant-*KCNQ1*/pcDNA3.1(+) and 1.25 μg of *KCNE1*/pcDNA3.1(+). Pulse protocol is shown in the inset on the top right.

showed much decreased amplitudes of currents compared to those of 0.625 μg of WT-*KCNQ1* (Fig. 3C).

The current–voltage relations of the peak current during depolarizing pulses and the tail current upon repolarization to −50 mV were summarized from pooled data in Fig. 4A and B. The current–voltage relations were almost similar in shape among 1.25 μg of WT-*KCNQ1*, 0.625 μg of WT-*KCNQ1* and 0.625 μg of WT-*KCNQ1* + mutant-*KCNQ1*, except for the current densities. The densities of the peak currents with 0.625 μg of WT-*KCNQ1* + *KCNE1* were nearly half of those with 1.25 μg of WT-*KCNQ1* at all test voltages (peak current at +60 mV; 16.6 ± 4.4 pA/pF, $n = 9$, and 34.5 ± 3.6 pA/pF, $n = 21$, respectively). The current densities with 0.625 μg of WT- + mutant-*KCNQ1* were significantly smaller than those with 0.625 μg of WT-*KCNQ1* (3.9 ± 2.3 pA/pF, $n = 5$, $p < 0.05$ vs 0.625 μg WT-*KCNQ1*; both contained *KCNE1*) (Fig. 4C). Thus, the current density generated by 0.625 μg of WT-*KCNQ1* + mutant-*KCNQ1* was equivalent to about 11% of the current induced by 1.25 μg of WT-*KCNQ1*. The densities of tail current from +60 mV test pulse were 6.4 ± 0.8 pA/pF in 1.25 μg of WT-*KCNQ1* ($n = 21$), 3.0 ± 1.1 pA/pF in 0.625 μg of WT-*KCNQ1* ($n = 5$) and 1.4 ± 0.4 pA/pF in 0.625 μg of WT-*KCNQ1* + mutant-*KCNQ1* ($n = 9$) (Fig. 4D). The results confirmed that the mutant-*KCNQ1* could suppress the function of WT-*KCNQ1* in a dominant-negative manner.

The voltage dependence of activation WT-*KCNQ1* (1.25 μg) gave in value (the $V_{0.5}$) of $+23.4 \pm 1.3$ mV and slope factor of 13.5 ± 1.2 mV ($n = 21$), which were fitted with Boltzmann function: $1[1 + \exp(V - V_{1/2})/k]$ (data not shown). These values were comparable to the findings in previous studies [5]. We could not analyze voltage dependence of activation or detailed kinetics of the mutant-*KCNQ1* with WT since extremely small current amplitudes made an accurate estimation result. However, the time courses of current activation during depolarizing

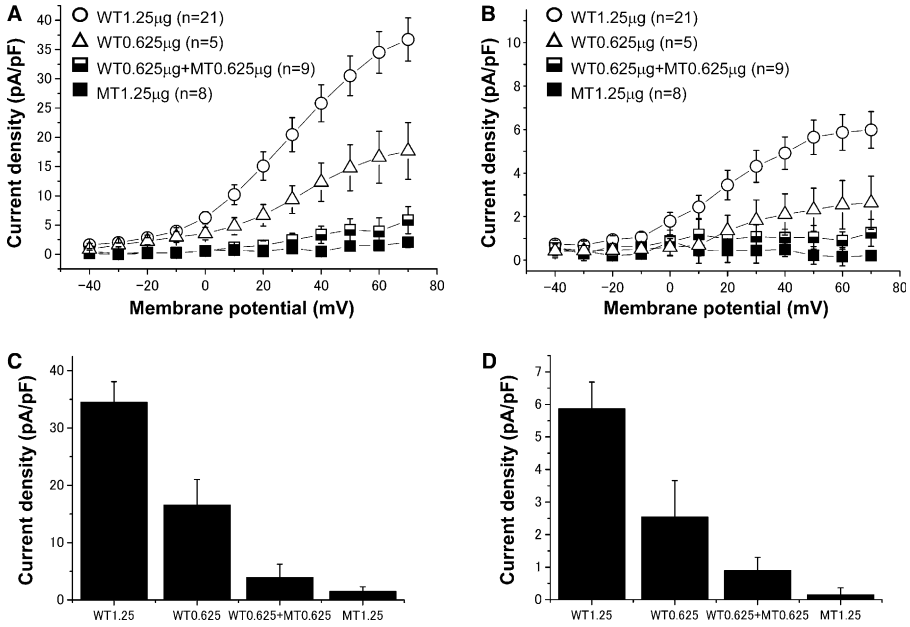

Fig. 4. Current–voltage relationships of expressed currents. (A) Current–voltage relationship measured at the peak current during test depolarization. (B) Current–voltage relationship measured at the tail current upon repolarization to −50 mV following test depolarization. (C) Bar graphs showing current densities obtained from the peak current at +60 mV. (D) Bar graphs showing current densities obtained from the tail current upon repolarization to −50 mV from +60 mV test depolarization.

pulses in WT- and mutant-*KCNQ1* appeared to be grossly similar to those in WT (see, Fig. 3C inset).

3.3. Expression of WT- and mutant-KCNQ1 channels in COS-7 cells

CFP-tagged WT-KCNQ1 channel was correctly distributed to the plasma membrane (Fig. 5A). On the other hand, the YFP-tagged mutant-KCNQ1 protein was retained in the cytoplasm and peri-nuclear space (Fig. 5B). Co-expression of CFP-tagged WT- and YFP-tagged mutant-*KCNQ1* demonstrated that the CFP signal was retained intracellular space, and the surface expression of CFP signal was significantly reduced (Fig. 6A), and the YFP signal (mutant channel) was retained in the cytoplasm (Fig. 6B). As shown in the merged image (Fig. 6C), CFP-tagged WT- and YFP-tagged mutant channel were co-localized suggesting that they formed complexes.

4. Discussion

We identified a novel *KCNQ1* mutation, Ala178fs/105, eliminating the S3–S6 and C-terminus portions of the channel in case of LQT patient. While the mutant-KCNQ1 alone failed to express functional channel, co-expression of WT- and mutant-KCNQ1 produced much decreased channel current compared to the same amount of WT-KCNQ1 channel alone, suggesting that the mutant-KCNQ1 suppressed the function of WT channel in a dominant-negative manner. Furthermore, the results indicate that the truncated mutant KCNQ1 formed hetero-tetramer with WT. The sub-cellular localization of the CFP- or YFP-tagged channel proteins actually revealed the intracellular retention of the mutant protein, as well as co-expressed WT and the mutant protein.

4.1. K-channel trafficking

Several different mutations in *KCNH2* were shown to cause trafficking defects, and the mutations were mostly missense mutations distributed in the C-terminus, although some missense mutations were located in the N-terminus, S5 or pore regions [6]. Especially in the case of KCNH2 channel, the C-terminal region including cyclic nucleotide binding domain is essential for channel trafficking, because it contains crucial sequence linked to the endoplasmic reticulum retention signal and the interaction site with GM130 required for channel protein trafficking [7]. On the contrary, the mechanism of channel trafficking in KCNQ1 channel was not well characterized because of rare incidence in the trafficking defect of this channel. Similar to KCNH2 channel, the C-terminal region of KCNQ1 channel may play a role in the channel trafficking, because Yamashita et al. reported that a missense mutation, Thr587Met, in the cytoplasmic region of KCNQ1 protein caused a trafficking defect [8].

4.2. Dominant-negative suppression

Dominant-negative suppression is one of the mechanisms for decreased current seen in the *KCNQ1* mutations to form hetero-multimer with WT [9]. The mutations in the pore region and in the supporting S5 transmembrane region of the KCNQ1 channel were thought to disrupt the potassium transport and associated with a dominant-negative effect [10,11]. The novel Ala178fs/105 mutation in *KCNQ1* described here was predicted to lack the S3–S6, pore, and C-terminal cytoplasmic regions. In transgenic mouse models, truncated N-terminal fragments of K channels were shown to exhibit a dominant-negative effect [12]. Furthermore, it is reported that the overexpression of another K channel gene compensate for the defective phenotype [13]. These observations suggested the importance of N-terminal region of KCNQ1 channel sup-

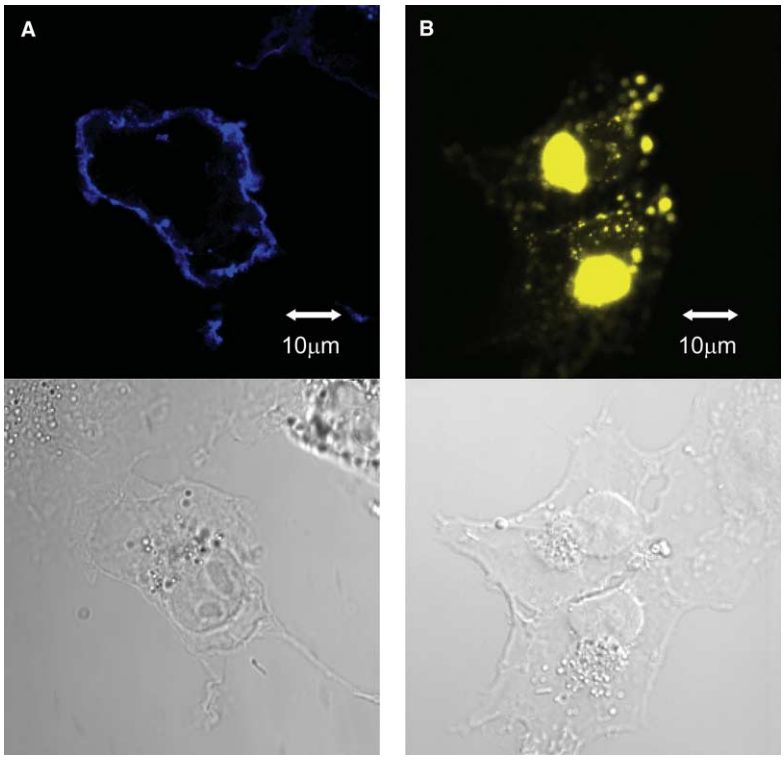

Fig. 5. Sub-cellular localization of WT- and mutant-KCNQ1 protein in COS-7 cells. Confocal microscopic images of CFP-tagged WT- and YFP-tagged mutant-KCNQ1 channel are presented. (A) Blue signals indicate CFP-tagged WT-KCNQ1 channel expressed on the cell surface. (B) Yellow signals indicate YFP-tagged mutant-KCNQ1 channel mainly expressed in the cytoplasm.

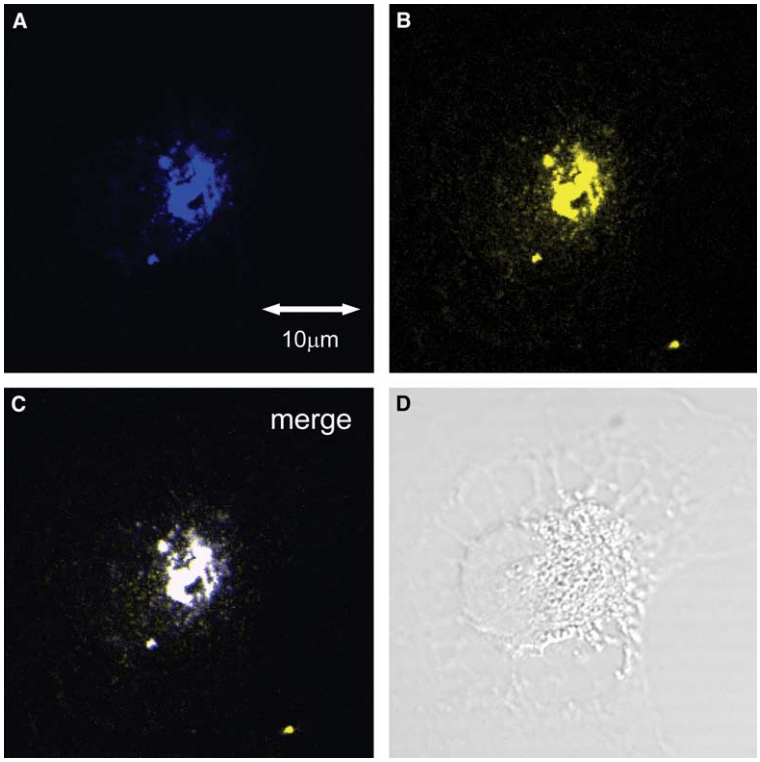

Fig. 6. Co-expression of WT- and mutant-KCNQ1 protein in COS-7 cells. (A) Co-expression of CFP-tagged WT-KCNQ1 and YFP-tagged mutant-KCNQ1 channel. CFP was visualized by 458 nm of Argon laser. WT-KCNQ1 channel (blue signals) was retained in the cytoplasm. (B) Co-expression of CFP-tagged WT-KCNQ1 and YFP-tagged mutant-KCNQ1 channel. YFP was visualized by 514 nm of Argon laser. The mutant-KCNQ1 channel (yellow signals) was retained in the cytoplasm. (C) Merged image of (A) and (B) demonstrates the co-localization of WT- and mutant-channels retained in the cytoplasm. (D) Transmitted light/DIC image of (A, B, C).

pressing the function of hetero-multimer in a dominant-negative manner.

Although detailed analysis for activation or inactivation kinetics of mutant-KCNQ1 channel was not achieved the time course of current activation and voltage dependency of WT- and mutant-*KCNQ1* (+*KCNE1*) appeared not much changed from those of WT (+*KCNE1*) (Fig. 3A and C). The results might indicate that decreased current amplitude is not caused by a failure of subunit interaction and/or homo- and hetero-multimeric assembly of the channel on the cell surface, but is caused by the trafficking defect of the channel protein as supported by the findings of the distribution of CFP- and YFP-tagged channels (Fig. 5). A trafficking defect as a mechanism for a dominant-negative suppression was reported by Ficker et al. [14].

4.3. KCNQ1 channel assembly

Our results provide another important aspect that the truncated KCNQ1 mutant lacking S3–S6 and C-terminus of the channel assembles with WT and conformed hetero-multimer. Schmitt et al. reported deletion of the carboxy-terminal subunit interaction domain (*sid*; residues 590–620) abolished functional channel expression and attenuated dominant-negative effect in co-expression studies [15]. The *sid* was also indicated as a determinant of the subunit specificity of KCNQ K^+ channel assembly [16]. The A178fs/105 mutant lacks the entire C-terminus including this presumed interaction domain, but it is able to assemble with WT causing a dominant-negative suppression. Our results may indicate the presence of another interaction site for subunit assembly in KCNQ1 subunit and the function of this site might be inhibited or inactivated by the interaction with some missing portion of this mutant. Otherwise additional 105 out of frame amino acid residues generated may play some role for channel assembly. These explanations are to be clarified by further studies.

Acknowledgements: The authors express their gratitude to Professor Jonathan Makielski (University of Wisconsin) for reading the manuscript. This work was supported by the Grants from the Ministry of Education, Science, Culture, Sports and Technology of Japan to AK and MH, and the Research Grant from the Ministry of Health, Labor and Welfare of Japan to AK, YA and MH.

References

[1] Kass, R.S. and Moss, A.J. (2003) J. Clin. Invest. 112, 810–815.
[2] Neyroud, N., Richard, P., Vignier, N., Donger, C., Denjoy, I., Demay, L., Shkolnikova, M., Pesce, R., Chevalier, P., Hainque, B., Coumel, P., Schwartz, K. and Guicheney, P. (1999) Circ. Res. 84, 290–297.
[3] Ho, S.N., Hunt, H.D., Horton, R.M., Pullen, J.K. and Pease, L.R. (1989) Gene 77 (1), 51–59.
[4] Wu, L.-M., Orikabe, M., Hirano, Y., Kawano, S. and Hiraoka, M. (2003) J. Cardiovasc. Pharmacol. 42, 410–418.
[5] Chouabe, C., Neyroud, N., Richard, P., Denjoy, I., Hainque, B., Romey, G., Drici, M.D., Guicheney, P. and Barhanin, J. (2000) Cardiovasc. Res. 45, 971–980.
[6] Thomas, D., Kiehn, J., Katus, H.A. and Karle, C.A. (2003) Cardiovasc. Res. 60, 235–241.
[7] Roti, E.C., Myers, C.D., Ayers, R.A., Boatman, D.E., Delfosse, S.A., Chan, E.K., Ackerman, M.J., January, C.T. and Robertson, G.A. (2002) J. Biol. Chem. 277, 47779–47785.
[8] Yamashita, F., Horie, M., Kubota, T., Yoshida, H., Yumoto, Y., Kobori, A., Ninomiya, T., Kono, Y., Haruna, T., Tsuji, K., Washizuka, T., Takano, M., Otani, H., Sasayama, S. and Aizawa, Y. (2001) J. Mol. Cell Cardiol. 33, 197–207.
[9] Vatta, M., Li, H. and Towbin, J.A. (2000) Curr. Opin. Cardiol. 15, 12–22.
[10] Shalaby, F.Y., Levesque, P.C., Yang, W.P., Little, W.A., Conder, M.L., Jenkins-West, T. and Blanar, M.A. (1997) Circulation 96, 1733–1736.
[11] Wollnik, B., Schroeder, B.C., Kubisch, C., Esperer, H.D., Wieacker, P. and Jentsch, T.J. (1997) Hum. Mol. Genet. 6, 1943–1949.
[12] Barry, D.M., Xu, H., Schuessler, R.B. and Nerbonne, J.M. (1998) Circ. Res. 83, 560–567.
[13] Brunner, M., Kodirov, S.A., Mitchell, G.F., Buckett, P.D., Shibata, K., Folco, E.J., Baker, L., Salama, G., Chan, D.P., Zhou, J. and Koren, G. (2003) Am. J. Physiol. Heart Circ. Physiol. 285, H194–H203.
[14] Ficker, E., Dennis, A.T., Obejero-Paz, C.A., Castaldo, P., Taglialatela, M. and Brown, A.M. (2000) J. Mol. Cell Cardiol. 32, 2327–2337.
[15] Schmitt, N., Schwarz, M., Peretz, A., Abitbol, I., Attali, B. and Pongs, O. (2000) EMBO J. 19, 332–340.
[16] Schwake, M., Jentsch, T.J. and Friedrich, T. (2003) EMBO Rep. 4, 76–81.